Frequency-Dependent Electrical Conductivity of CVD-Grown ZnSe Polycrystals: Analysis Based on Jonscher's Universal Power Law

I. I. Abbasov[1*], M. A. Musaev[1],
J. I. Huseynov[2], R. B. Aslanov[3], and
E. A. Eminova[1]

[1]Azerbaijan State Oil and Industry University, Baku, Azerbaijan
ibrahimabbasov179@gmail.com
[2]Azerbaijan State Pedagogical University, Baku, Azerbaijan
jahangirhuseynov1958@gmail.com
[3]Institute of Biophysics, Ministry of Science and Education of the Republic of Azerbaijan, Baku, Azerbaijan

Abstract. The structural, vibrational, and electrical properties of ZnSe crystals grown by chemical vapor deposition (CVD) were investigated. X-ray diffraction analysis confirmed the formation of high-quality cu- bic sphalerite ZnSe with pronounced (111) crystal texture, submicron crystallite size, and high structural homogeneity. Elemental composition analysis revealed near-stoichiometric ZnSe with minor selenium excess, while Raman spectroscopy identified well-defined transverse (TO) and longitudinal (LO) optical phonon modes, indicating low structural disor- der. Impedance spectroscopy showed that the electrical conductivity of ZnSe polycrystals exhibits frequency-dependent dispersive behavior, con- sistent with hopping conduction of localized carriers. The results demon- strate that CVD-grown ZnSe crystals possess high structural and chem- ical quality and are promising materials for optoelectronic applications.

Keywords: chemical vapor deposition (CVD), X-ray diffraction, Raman spectroscopy, electrical conductivity, optical phonons, optoelectronic materials.

1 Introduction

Binary compounds of the II–VI group elements, known as A_2B_6-type semicon- ductors (ZnS, ZnSe, CdS, CdSe, CdTe, etc.), represent one of the primary objects of study in modern semiconductor physics. In these compounds, covalentionic bonds are formed between group II metals (Zn, Cd, Hg) and group VI chalcogens (S, Se, Te), which determine both their chemical and physical properties. The lattice structure of A_2B_6-type crystals is typically cubic or hexagonal, defining the crystal symmetry and the degree of optical anisotropy [1–3].

R. Rzayev et al. (eds.), *Proceedings of the International Conference on Current Problems in Engineering and Applied Sciences (ICCPEAS 2025)*, Advances in Engineering Research 299,
https://doi.org/10.2991/978-94-6239-668-5_25

These semiconductors exhibit a wide bandgap ($E_g \approx 2$–3.8 eV), high dielectric constant, large exciton binding energy, and high radiation resistance. Such properties make them essential base materials for the fabrication of optoelectronic devices operating in the ultraviolet and visible ranges, including light emitting diodes (LEDs), laser diodes, photodetectors, solar cells, and electrooptic modulators [4–6]. The physical properties of A_2B_6 compounds are closely related to both lattice defects and the type and concentration of impurity dopants. These parameters significantly influence electrical conductivity, photoluminescence spectra, and carrier recombination kinetics.

In recent years, obtaining A_2B_6 type compounds in nanostructured forms such as thin films, quantum dots, and nanocrystals has greatly expanded their application potential. Due to size effects and surface quantization, the bandgap in such structures widens, enabling control over their spectral properties. Thus, A_2B_6- type compounds are not only fundamental objects of semiconductor physics research but also promising materials for the development of high efficiency and environmentally friendly optoelectronic devices [7–9].

In contemporary electronic and optoelectronic technologies, zinc selenide (ZnSe) crystals of the A_2B_6 type are of particular importance. These materials possess superior characteristics, including high electrical resistivity, low dielectric losses, mechanical stability, radiation resistance, and environmental robustness. ZnSe crystals are transparent in the 0.6–20 μm range and are widely used in CO_2 laser optics, infrared systems, thermal imaging, and night vision devices [10–12].

Investigating the frequency and temperature dependence of certain electrophysical properties of ZnSe crystals under varying electric fields holds significant scientific and practical relevance for modern semiconductor physics and optoelectronics. Studying the laws governing the variation of electrical conductivity, dielectric constant, and relaxation processes with temperature and frequency allows clarification of carrier kinetic mechanisms and the nature of defect structures. Research in this area provides a theoretical and practical basis for improving high frequency and high temperature optoelectronic devices, infrared detectors, electrooptic modulators, and thin film technologies. The present paper is devoted to the scientific analysis of these pertinent issues and to the investigation of the electrical conductivity of ZnSe crystals obtained via the CVD method.

2 Experimental Methodology

Although high-purity ZnSe crystals can be grown using various methods, the CVD (Chemical Vapor Deposition) technique is distinguished by its structural and optical homogeneity. This method allows precise control over growth parameters (temperature, pressure, and reactant flow), ensuring the production of high quality, mechanically robust, and smooth surfaced crystals. The ZnSe crystals investigated in this study were synthesized by the CVD method using zinc and hydrogen selenide vapors.

Polycrystalline CVD-ZnSe is obtained via chemical vapor deposition in a reactor.

Deposition occurs on a graphite substrate from zinc and hydrogen selenide (H_2Se) vapors in a flow system with a continuous supply of reactants diluted in a carrier gas (argon). The zinc evaporation rate is controlled by adjusting the temperature of the reactor's working zone (600–800 °C, <100 torr). Zinc and H_2Se vapors, prediluted with argon, are mixed in the deposition zone. The reactor is made of chemically inert and heat resistant material that does not adhere to ZnSe. Graphite plates are used as substrates, on which a thin layer of graphite powder is applied to reduce adhesion.

The X-ray diffraction (XRD) pattern of the CVD ZnSe sample was recorded using a Miniflex 600 X-ray diffractometer. The morphology and microstructure of the sample surface were examined using a Japanese made JEOL JSM6610- LV scanning electron microscope (SEM). Quantitative X-ray microanalysis was employed to determine the phase composition and the distribution of chemical elements on the sample surface.

Raman scattering spectra were measured using a confocal Raman microspec- trometer Nanofinder 30 (Tokyo Instruments, Japan). An Nd:YAG laser with a wavelength of 532 nm and a maximum output power of 10 mW was used as the excitation source. The spectral resolution was no worse than 0.5 cm^{-1}. The scattered radiation was detected with a thermoelectrically cooled CCD camera (1024 × 128 pixels), operating in photon counting mode. The frequency dependence of the electrical conductivity of the samples was investigated using a high-precision impedance analyzer Keysight E4990A, operating in the frequency range from 20 Hz to 120 MHz [13]. This device allows measurement of the complex impedance $Z^* = R + jX$, from which conductivity parameters and dielectric properties of the material are calculated.

For the experiment, the samples were prepared in the form of pressed pellets placed between two flat electrodes, forming a capacitor-like cell. Contact between the electrodes and the sample surfaces was ensured by applying a thin layer of silver paste, minimizing contact resistance. Measurements were conducted under an alternating voltage of 0.5–1 V applied to the sample.

During the measurement, the instrument recorded current and voltage values, from which the complex impedance Z^* was calculated. Subsequently, the complex admittance $Y^* = \frac{1}{Z^*} = G + jB$ and the real part of the conductivity (G), characterizing the actual electrical conductivity of the material, were determined.

3 Results and Discussion

The ZnSe compound exists in two modifications: cubic (sphalerite, B3 type, space group F43m) and hexagonal (wurtzite, B4 type, $P6_3mc$). The stable form is the cubic sphalerite modification, whereas the wurtzite phase arises as metastable during gas phase crystallization or decomposition of zinc organic compounds.

The X-ray diffraction (XRD) pattern shows one very high and narrow peak around ~27–28° (2θ). For cubic ZnSe, this corresponds to the (111) plane. Such a dominant peak

indicates that a large portion of the sample volume is oriented in the same direction effectively a textured or pseudo dominant unidirectional growth (directional crystallization during CVD).

In the XRD pattern of CVD-grown ZnSe crystals, three characteristic diffrac- tion maxima are observed (Fig. 1) at $2\theta \approx 27.2^{\circ}$, 45.2°, and 53.6°, corresponding to the (111), (220), and (311) reflection planes of the cubic sphalerite lattice (space group F43m), which is characterized by a face centered cubic (FCC) lattice. The main intense peak at $2\theta \approx 27.2^{\circ}$ indicates a pronounced crystal texture in the (111) direction. Comparison of the experimental data with the reference pattern (JCPDS No. 00-065-9603) confirms the formation of the cubic ZnSe phase without any secondary phases. Calculation of the interplanar distances and lattice parameter using Bragg's law gave $a \approx 5.666$ Å, which is in good agreement with literature data for ZnSe, indicating high structural perfection of the obtained samples. Crystallite sizes, calculated using the Scherrer formula from the half-widths of the diffraction peaks, are on the order of $(4.5\tilde{}5.5) \times 10^2$ nm, indicating a submicron grain size and a high degree of crystallinity. The narrow peaks and absence of spurious reflections suggest a low level of internal strain and high homogeneity of the CVD grown ZnSe crystal structure. These results confirm that the chosen synthesis parameters provide crystalline or weakly textured ZnSe samples with good structural quality.

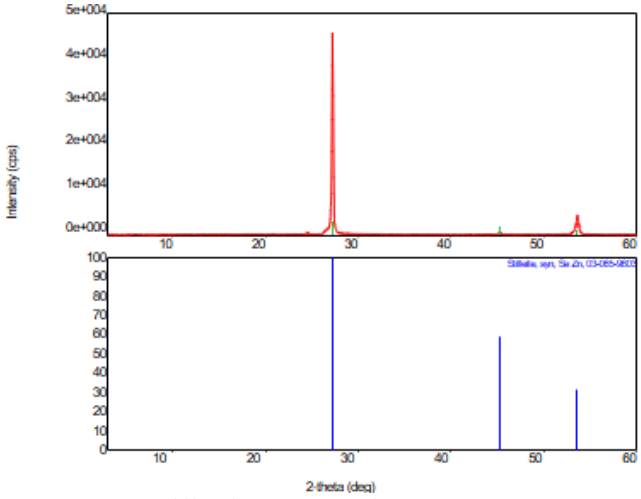

Fig. 1. Diffraction patterns of CVD ZnSe.

Morphology and surface elemental composition analysis revealed high homogeneity with minor deviations in stoichiometry within the ZnSe homogeneity region towards a selenium excess (Fig. 2). The spectrum clearly identifies lines belonging to zinc (Zn K) and selenium (Se L), confirming the formation of the binary ZnSe compound without foreign inclusions. The atomic concentration ratio Zn:Se ≈ 48.78:51.22, which is close to

the stoichiometric 1:1 composition. The slight excess of selenium may be associated with specific deposition process characteristics or surface enrichment of Se during CVD growth.

No extraneous peaks are observed in the spectrum, indicating the absence of impurities and high chemical purity of the obtained crystals. This suggests that the applied CVD technology ensures the production of homogeneous and chemically pure ZnSe crystals with a nearly ideal stoichiometric composition.

Additional studies using a scanning electron microscope with microanalysis capability (REMMA-102-02, Fig. 2) revealed local regions with a zinc excess. Thus, it was established that the ZnSe homogeneity region is bidirectional. Depending on the synthesis conditions zinc or selenium excess it is possible to obtain ZnSe samples with either electronic (n-type) or hole (p-type) conductivity [14]. Raman spectroscopy (RS) was performed to investigate the vibrational and structural properties of ZnSe. As is known, the ZnSe crystal contains two atoms in the primitive unit cell, resulting in six vibrational modes three acoustic and three optical. Since the ZnSe unit cell possesses cubic symmetry, the optical vibrations are characterized by a triply degenerate F_2 mode, which splits into longitudinal (LO) and transverse (TO) phonon modes [15, 16].

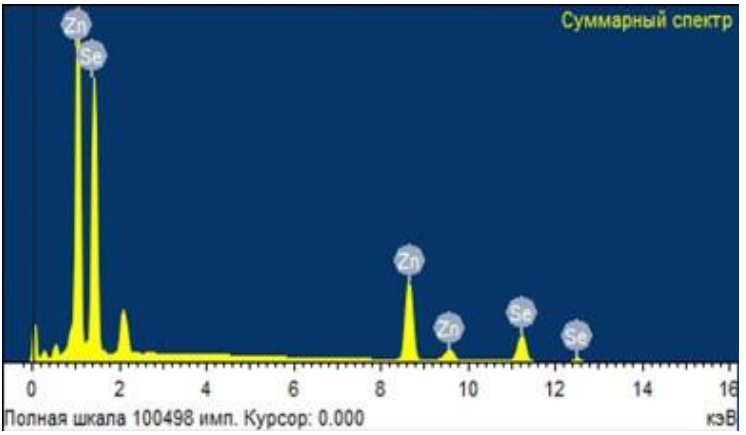

Fig. 2. X-ray microanalysis of the surface of CVD ZnSe crystals.

Figure 3 shows the obtained ZnSe Raman scattering spectra. Analysis of the spectra reveals the presence of transverse (TO) and longitudinal (LO) optical phonon modes. Based on the experimentally obtained Raman spectra of polycrystalline CVD ZnSe samples, three prominent scattering bands were identified at approximately 160, 195, and 246 cm^{-1}. The peak near 195 cm^{-1} is unambiguously attributed to the transverse optical (TO) mode of the ZnSe crystal lattice. This value is in good agreement with the tabulated TO phonon frequen- cies of the sphalerite modification of ZnSe. Meanwhile, the intense band around 246 cm^{-1} corresponds to the longitudinal optical (LO) mode. The

simultaneous presence of well-defined TO and LO modes indicates the high crystalline quality of the CVD films and a low level of structural disorder.

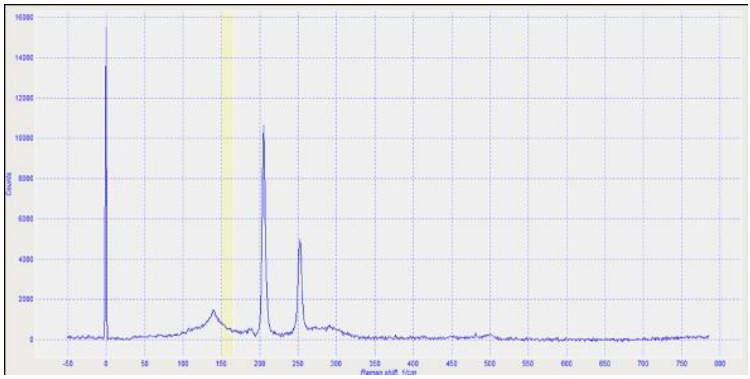

Fig. 3. Diffraction patterns of CVD ZnSe.

A broad and relatively weak feature in the region of ≈150–165 cm^{-1} has a different origin. Since fundamental single-phonon modes do not exist in this range for an ideal cubic ZnSe lattice, this band is most likely associated with multiphonon processes or local vibrations related to defects, grain boundaries, and short range order disruptions typical for polycrystalline CVD structures.

During measurements based on impedance spectroscopy, the frequency and temperature dependence of the electrical conductivity and dielectric permittivity of the samples were determined.

As seen from the graph (Fig. 4), in the frequency range $\log(f) \approx 1.3$˜7.4, the specific electrical conductivity of CVD ZnSe polycrystals exhibits an exponential increase, approximately in the range of 10^{-8}–10^{-2} S/m. The graph can be divided into three regions:

1. Low-frequency region ($\log f < 4$): conductivity values are very small, with only a slight increase. Electrical conductivity is limited by slow relaxation of ions and trapped carriers.
2. Intermediate frequency region ($4 < \log f < 6$): the increase in conductivity ace lerates. The hopping conduction mechanism becomes dominant.
3. High-frequency region ($\log f > 6$): conductivity rises sharply to approximately 10^{-5}–10^{-2} S/m. Free charge carrier motion synchronizes with the alternating field, producing dispersive conductivity.

The increase in conductivity follows Jonscher's empirical law:

$$\sigma(\omega) = \sigma_{dc} + A\omega^{s}, \qquad 0 < s < 1 \qquad (1)$$

where σ_{dc} is the direct current conductivity, A is a constant, and s is the frequency exponent.

Fitting yields:

$$\sigma_{dc} = 1.55 \times 10^{-8}\ \text{S m}^{-1}, \qquad A = 4.48 \times 10^{-11}\ \text{S m}^{-1}\text{Hz}^{-s}, \qquad s = 0.94.$$

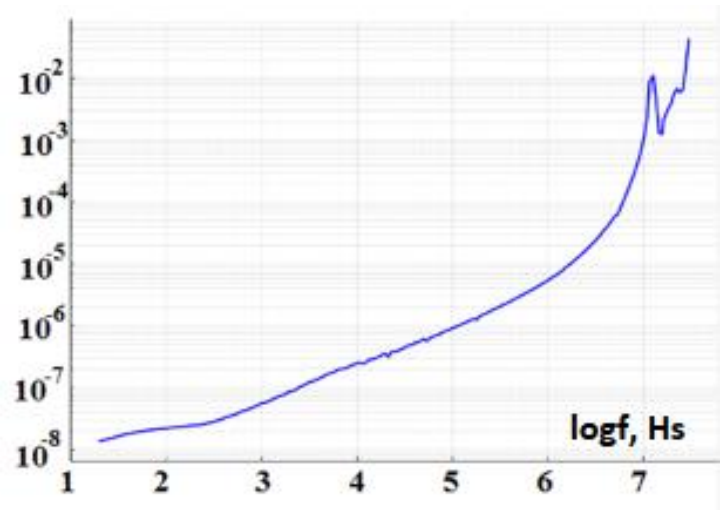

Fig. 4. Frequency dependence of electrical conductivity of CVD ZnSe polycrystals.

At low frequencies, conductivity remains constant and eqSSuals σ_{dc}, indicating hopping conduction between localized states. With increasing frequency, the rise in $\sigma(f)$ is associated with dipolar relaxation and energetic transitions of localized carriers.

The relatively small A parameter indicates weak dispersive conductivity, typical for semiconductor crystalline systems. The obtained results confirm that CVD grown ZnSe polycrystals exhibit frequency dependent dispersive conductivity and are promising for applications in devices with frequency controllable electrical properties.

4 Conclusion

The comprehensive structural, vibrational, and electrical characterization of CVD-grown ZnSe demonstrates that the applied synthesis route yields highquality polycrystalline material with well-defined cubic sphalerite structure. XRD analysis confirmed the formation of a phase-pure ZnSe lattice with pronounced (111) texture and a lattice parameter consistent with reference data, indicating high structural order and low internal strain. SEM EDS studies revealed a composition close to the ideal 1:1 stoichiometry with slight local deviations toward Zn or Se rich regions, suggesting a bidirectional homogeneity range typical for ZnSe. Raman spectroscopy further supported the structural integrity of the samples by identifying well-resolved TO and LO phonon modes, while the presence of a weak broad band near 150–165 cm^{-1} was attributed to defect-induced or multiphonon

vibrational processes common in polycrystalline CVD films. Electrical measurements based on impedance spectroscopy established that the conductivity of ZnSe exhibits a pronounced frequency dispersion consistent with Jonscher's universal relaxation law. The material demonstrates low dc conductivity associated with localized charge carriers and a transition to hopping dominated conduction at higher frequencies. The extracted parameters (σ_{dc}, A, and s) reflect weak carrier localization and an energetically favorable structure for frequency-activated charge transport. Overall, the results confirm that CVD-grown ZnSe combines high crystallinity, near stoichiometric composition, and stable dielectric and electrical behavior, making it a promising candidate for high-performance optoelectronic and frequency-sensitive device applications.

References

1. P.Y. Yu, M. Cardona, *Fundamentals of Semiconductors: Physics and Materials Properties*, Springer Science & Business Media, pp. 778 (2010)
2. S.-H. Wei, A. Zunger, Calculated Natural Band Offsets of all II–VI and III–V Semi-conductors: Chemical Trends and the Role of Cation d Orbitals, *Applied Physics Letters* 72(16), 2011–2013 (1998).
3. J. Mao, W. Xu, S. Seo, Exploring the dual phases of cadmium sulfide: synthesis, properties, and applications of hexagonal wurtzite and cubic zinc blende crys- tal structures, *Journal of Materials Chemistry A* 12, 23218–23242 (2024).
4. J. Wang, Y. Xing, F. Wan, et al., Progress in ultraviolet photodetectors based on II–VI group compound semiconductors, *Journal of Materials Chemistry C* 10, 12929–12946 (2022). DOI:
5. I. Nasieka, V. Strelchuk, P. Fochuk, et al., Increased radiation hardness of detector-grade $Cd_{0.96}Zn_{0.04}Te$ crystals by doping with In and Ge, *Radiation Physics and Chemistry* 165, 108448 (2019).
6. J. Jie, W. Zhang, I. Bello, et al., One-dimensional II–VI nanostructures: Synthesis, properties and optoelectronic applications, *Nano Today* 5(4), 313–336 (2010).
7. B.T. Diroll, B. Guzelturk, H. Po, et al., 2D II–VI Semiconductor Nanoplatelets: From Material Synthesis to Optoelectronic Integration, *Chemical Reviews* 123(7), 3543–3624 (2023).
8. A. Bukhtiar, B. Zou, Low-dimensional II–VI semiconductor nanostructures of ternary alloys and transition metal ion doping: synthesis, optical properties and ap- plications, *Materials Advances* 5, 6739–6795 (2024).
9. J. Llusar, I. du Fossé, Z. Hens, A. Houtepen, I. Infante, Surface Recon- structions in II–VI Quantum Dots, *ACS Nano* 18(2), 1563–1572 (2024).
10. V. Mittal, N.P. Sessions, J.S. Wilkinson, G.S. Murugan, Optical quality ZnSe films and low loss waveguides on Si substrates for mid-infrared applications, *Optical Materials Express* 7, 712–725 (2017).
11. H. Qi, X. Zhang, M. Jiang, Q. Wang, Optical Constants of Zinc Selenide in Visible and Infrared Spectral Ranges, *Journal of Applied Spectroscopy* 84(4), 1–4 (2017).
12. F.E. Alam, B. Ali, S. Arif, Electric field and strain mediated zinc blende ZnSe: ex- ploring its potential as a controlled stimulus responsive optical and optoelectronic material, *Materials*

Advances 5, 9656–9672 (2024).
13. A.E. Nabiyev, J.I. Huseynov, I.I. Abbasov, Dielectric properties of $Ba_{0.8}Sr_{0.2}TiO_3$ ferroelectric films in an alternating electric field, *Canadian Journal of Physics* 102(6), 325–331 (2024).
14. M. Scepanovica, M. Grujic-Brojcina, D. Nesheva, Z. Levi, I. Bineva, Z.V. Popovic, Characterization of ZnSe nanolayers by spectroscopic ellipsometry, *Acta Physica Polonica A* 116(4), 708–711 (2009).
15. M. Liu, P. Duan, M. Shafi, W. Liu, W. Zhang, C. Zhang, X. Hu, J. Gao, C. Zhang, Surface-enhanced Raman spectroscopic activity study on topo- logical ZnSe nanostructures, *Frontiers in Physics* 10, 1057992 (2022).
16. M.S. Afanasiev, E.I. Goldman, G.V. Chucheva, et al., Conductivity of Metal–Dielectric–Semiconductor Structures Based on Ferroelectric Films, *Physics of the Solid State* 62, 164–167 (2020).
17. I. Abbasov, M. Musayev, J. Huseynov, et al., Temperature behavior of X-ray luminescence spectra of ZnSe, *International Journal of Modern Physics B* 36(02), 2250018 (2020).